A Novel Predictive Control Scheme for Interleaved Buck Converter in Low Power Applications

Mahesh Babu Tirumalasetti[1], Udaya Bhasker Manthati[1], Punna Srinivas[2] and C. R. Arunkumar[1,*]

[1]*Department of Electrical Engineering, National Institute of Technology, Warangal, Telangana-506004, India*
[2]*Electrical Engineering Department, BVRIT HYDERABAD College Engineering for Women, Hyderabad, Telangana-500090, India*
E-mail: tiruma_ee19425@student.nitw.ac.in; ub@nitw.ac.in; srinivas.p@bvrithyderabad.edu.in; acr_research@student.nitw.ac.in
[*]*Corresponding Author*

Received 29 June 2021; Accepted 20 November 2021;
Publication 16 February 2022

Abstract

This paper presents a model predictive control (MPC) approach for Interleaved Buck Converter in low power applications. Traditional PI-based control strategies have an arduous tuning process and can affect its performance when there are fluctuations in the operating point. Therefore, an MPC-based control strategy is proposed because of its simplicity, intuitiveness, ease of implementation, and inclusion of nonlinearities and constraints. Firstly, the model of Interleaved Buck Converter (IBC) is developed. Secondly, a two-loop control strategy is developed with predictive inner current control and outer voltage control for DC link voltage regulation. In comparison to traditional control strategies, the proposed one has a better dynamic response. Finally, simulation studies are done using MATLAB Simulink, and

Distributed Generation & Alternative Energy Journal, Vol. 37_3, 609–630.
doi: 10.13052/dgaej2156-3306.37311
© 2022 River Publishers

a prototype experimental setup is developed to validate the effectiveness of the proposed control strategy in the dSPACE1104 platform.

Keywords: Model predictive control, proportional integral control, interleaved buck converter, multiphasing.

1 Introduction

Interleaving, also known as multiphasing, is a technique for shrinking the size of a filter part. There will be N number of power switches in the interleaved circuit. The switches have a phase gap of $\frac{360°}{N}$. The interleaving technique is a strategic interconnection of multiple switching cells that enhances the effective pulse frequency by aligning and operating multiple smaller sources with a relative phase shift [1]. The power scale and conducted electromagnetic emission of the converter are all improved by using an interleaved process. Harmonic cancellation, increased efficiency, improved thermal performance, and a high-power density can all be achieved with interleaving [2].

With a conventional buck converter converting high voltage to low voltage, a short duty cycle is required, which adds several limitations to the various components and trigger circuitry, and usually requires relatively high values of inductance and capacitor to ensure allowable current and voltage ripple within limits. Problems with high-level converters are presented in [3, 4]. So, the interleaved converter is the solution to overcome the drawbacks of conventional converters [5]. Interleaved buck converters are used in dc systems for regulated power applications such as various microcontroller power supplies [6], solar energy harvesting [7], LED lighting systems [8], automotive systems [9], and pulse power supplies [10]. State-space modeling, average modeling, and current sharing problems among inductors in interleaved converters address in [11–16]. An interleaved buck converter for driving high-brightness LEDs is briefly mentioned in [17–19].

The PI-based control strategy for IBC is proposed in [20]. However, these PI-based dual-loop control strategies cannot provide a desirable transient response; indeed, they often result in a short settling period with a high overshoot or a low overshoot with a long settling time. It is difficult to tune a PI controller since tuning of a PI controller needs system modeling and linearization around an operating point to derive transfer functions and its performance will be affected when the operating point varies [21, 22]. There are three loops and six parameters to tune in a PI-based control strategy, which complicates the controller design process [23].

MPC is a promising new technique that uses a discrete model of the system and current states of the system to predict future states and determine the best control action to take at each sampling moment. MPC improves the system's robustness by dealing with possible interference, noise, and other factors [24]. MPC-based control strategies for different converters are proposed in [25–29]. The MPC method proposed in [25, 26] involves operations of several matrices, resulting in a large computational time and complexity. To overcome this [27–29] have proposed a relatively low complex MPC control strategy with dynamic reference generation. A MPC control strategy for an Interleaved Buck Converter for DC link voltage regulation is proposed in this paper. The paper discusses the following contributions.

- A two-loop control structure with an outer voltage loop that generates dynamic references and an inner current control loop that allows for reference splitting without low pass filters and reference tracking utilizing MPC principles.
- Equally distribute load current stress and feed less ripple current through the load.
- Improved dynamic output over the standard PI-based system.

The rest of the paper presents system configuration, proposed MPC control strategy, simulation results, experimental results and conclusion.

2 System Configuration

2.1 Circuit Diagram of IBC

The circuit diagram of IBC with controller is shown in Figure 1, consists of two buck converters connected in parallel with a common source V_{in} and

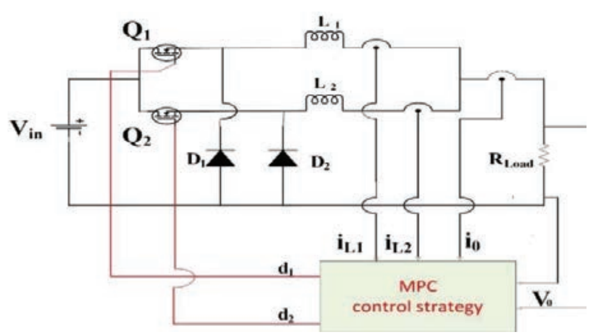

Figure 1 Block diagram of interleaved buck converter.

Table 1 Modes of operation

Modes of Operation	Switch (Q_1)	Switch (Q_2)	Diode (D_1)	Diode (D_2)
Mode I	ON	OFF	OFF	ON
Mode II	OFF	OFF	ON	ON
Mode III	OFF	ON	ON	OFF
Mode IV	OFF	OFF	ON	ON

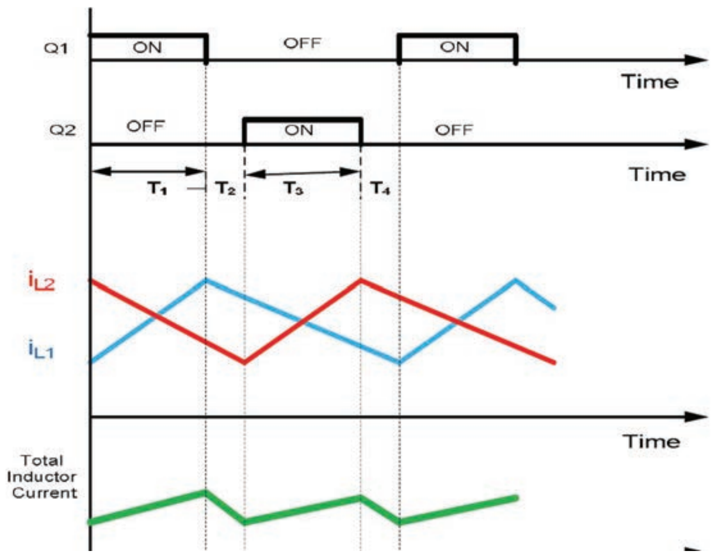

Figure 2 Steady state inductor current waveforms.

common load (R_{Load}). IBC's key components are switches Q_1, Q_2, diodes D_1, D_2, and inductors L_1, L_2. The operation of IBC is split into four modes. Table 1 shows the state of the switches and diodes in each mode. Figure 2 depicts the steady-state inductor current waveforms of IBC.

2.2 Modes of Operation

In mode I ($\mathbf{0} < \mathbf{t} < \mathbf{T_1}$), switch ($Q_1$) is on by applying gate pulse and switch (Q_2) is off. So, inductor current i_{L1} increases with a slope of $\frac{(V_{in}-V_0)}{R}$ and inductor current i_{L2} freewheels through load and (D_2) with a slope of $\frac{-V_0}{R}$. In mode II ($\mathbf{T_1} < \mathbf{t} < \mathbf{T_2}$), both switches ($Q_1$) and ($Q_2$) are off. So, both inductor currents i_{L1} and i_{L2} freewheels through load and their respective diodes (say D_1 or D_2). In mode III ($\mathbf{T_2} < \mathbf{t} < \mathbf{T_3}$), switch ($Q_1$) is off and switch ($Q_2$) is on by applying a gate pulse to it. So, inductor current i_{L1}

freewheels through load and D_1 with a slope of $\frac{-V_O}{R}$ and inductor current i_{L2} rises with a slope of $\frac{(V_{in}-V_0)}{R}$.

In mode IV $(\mathbf{T_3} < \mathbf{t} < \mathbf{T_4})$, again both switches are off. So, both inductor currents i_{L1} and i_{L2} freewheels through load and their respective diodes (say D_1 or D_2). In all four modes, total load current (i_0) is supplied by both inductor currents i_{L1} and i_{L2}. Hence interleaving converters reduces the burden on the components of the converters. So, the size of the converters decreases with interleaving. And also, by controlling inductor currents proper load sharing is achieved.

3 Proposed MPC Control Strategy

As shown in Figure 3, the conventional control has three PI controllers. So, a total of six parameters are tuned to get the desired output. These six parameters are difficult to tune. The proportional gain (Kp) and the integral gain (ki) of the PI controller depend on the system parameters and are need to be pre-calculated. The major disadvantages of PI controllers are the constraints cannot be included and the controller design becomes more complicated for multivariate systems.

The proposed control system is shown in Figure 4. MPC uses the discrete model of the system for control action. It uses the current state of the system and considers the effect of present actions on future outputs. The MPC controller output is a solution to an explicit optimization problem. The objective function of the optimization problem encapsulates the required control strategy. MPC controllers solve the optimization problem at each sampling interval.

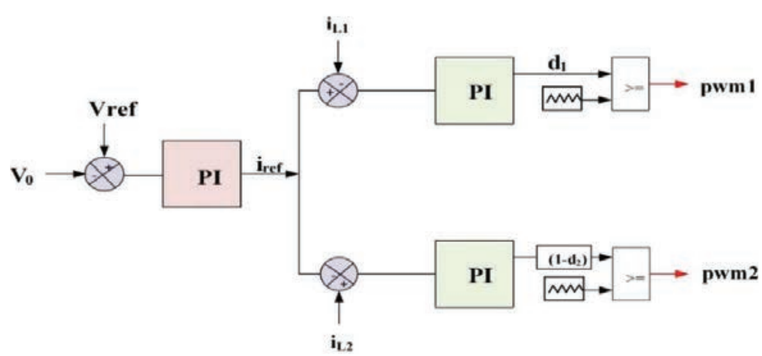

Figure 3 The conventional PI control strategy.

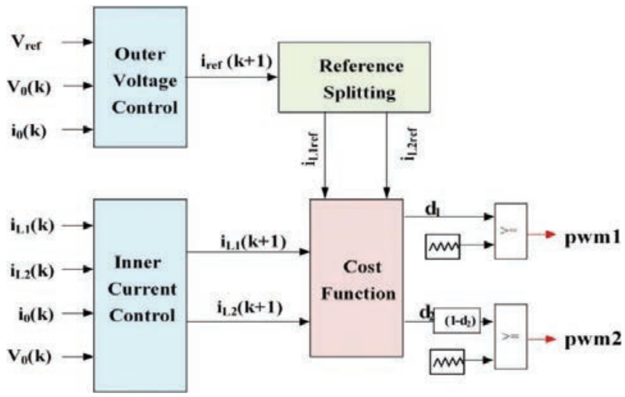

Figure 4 The proposed MPC control strategy.

The proposed system as shown in Figure 4 has two parts.

- Dynamic reference current calculation to be supplied for DC link voltage regulation.
- Prediction of inductor currents from a discrete model of DC/DC converter and generation of modulating signals that ensures the least error between predicted and reference values.

3.1 Dynamic Reference Calculations

The current through the DC link capacitor is given by the Equation (1) the change the V_0 will be directly affected by i_c the charging current.

$$i_c = C_0 \frac{dV_0}{dt} \tag{1}$$

By expanding the above equation by Euler's difference law for a small sampling period we get

$$i_c(k) = C_0 \frac{V_0(k) - V_0(k-1)}{T_s} \tag{2}$$

Where T_s denotes the sampling period $V_0(k)$ denotes the present sampled value and $V_0(k-1)$ denotes the previous sampled value.

$$i_c(k+1) = C_{\mathbf{0}} \frac{V_0(k+\mathbf{1}) - V_{\mathbf{0}}(k)}{T_s} \tag{3}$$

for $V_0(k+1)$ to be V_{ref} the calculated $i_c(k+1)$ value from the above equation will be large initially to limit this value an integer coefficient N as a prediction horizon is introduced such that

$$\mathrm{i_c(k+1) = C_0 \frac{V_{ref} - V_0(k)}{N \times T_s}} \tag{4}$$

Now the total reference current to be supplied for DC link voltage regulation is given by

$$\mathrm{i_{ref}(k+1) = i_c(k+1) + i_0(k)} \tag{5}$$

Here $\mathrm{i_0(k)}$ is the load current.

3.2 Predictive Current Control

For the prediction of inductor currents an averaged voltage balance equation across these inductors is developed. For $\mathrm{L_1}$ below equation is derived

$$L_1 \frac{di_1}{dt} = (V_{in} - V_o)d_1 - V_o(1 - d_1) \tag{6}$$

Expanding using euler's difference law

$$L_1 \frac{i_1(k+1) - i_1(k)}{T_s} = \{V_{in}(k) - V_o(k)\}d_1(i) - V_o(k)(1 - d_1(i)) \tag{7}$$

From the above equation $iL_1(\mathrm{k}+1)$ is calculated

$$i_{L1}(k+1) = \frac{T_s}{L_1} \times [\{V_{in}(k) - V_o(k)\}d_1(i) - V_{dc}(k)(1 - d_1(i))] + i_1(k) \tag{8}$$

Similarly, another inductor current model is derived as follows

$$\mathrm{L_2 \frac{di_2}{dt} = (-V_o)d_2 + (V_{in} - V_o)(1 - d_2)} \tag{9}$$

From the above equation $iL_2(\mathrm{k}+1)$ is derived as

$$\mathrm{i_{L2}(k+1) = \frac{T_s}{L_2} \times [-V_o(k)d_2(j) + V_{in}(k) - V_o(k)(1 - d_2(j)) + i_2(k)} \tag{10}$$

The cost functions for $\mathrm{i_{L1}}$ and $\mathrm{i_{L2}}$ current control are

$$\mathrm{J_1 = i_{L1ref}(k+1) - i_{L1}(k+1))^2} \tag{11}$$

$$\mathrm{J_2 = i_{L2ref}(k+1) - i_{L2}(k+1))^2} \tag{12}$$

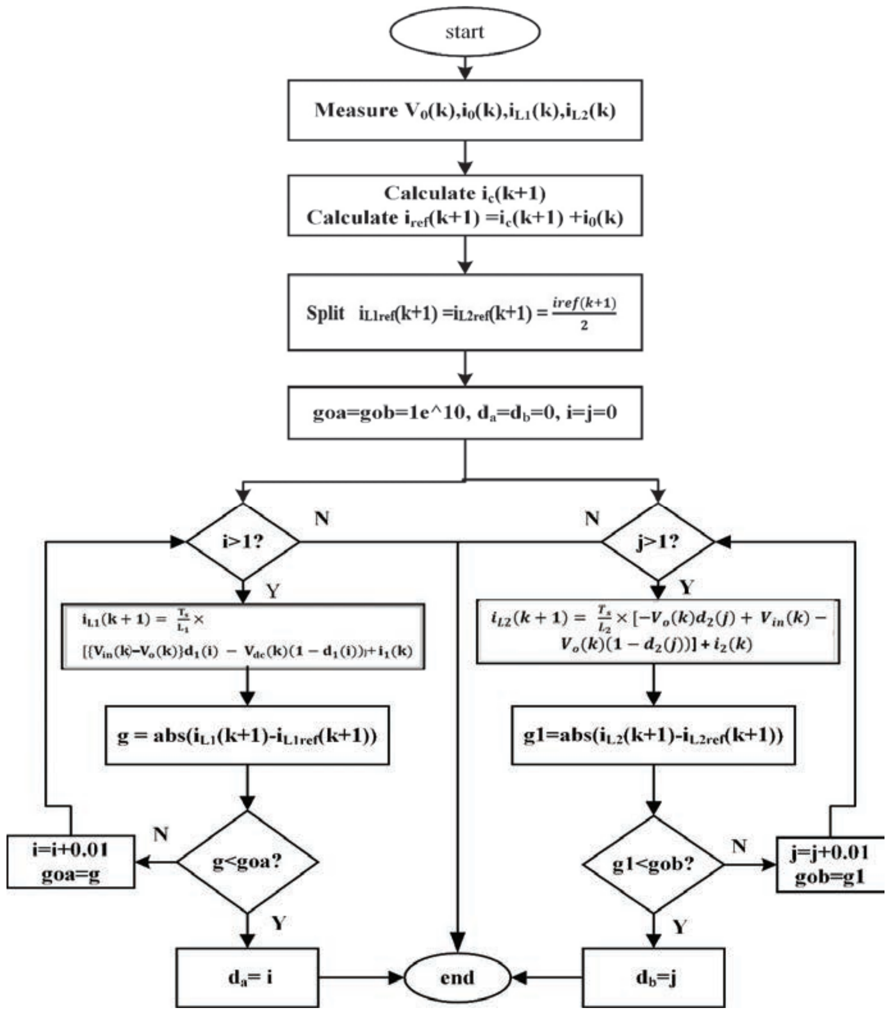

Figure 5 Working of MPC controller.

Equation (8), (10) are iteratively calculated for d_1 and d_2 from 0 to 1 with an increment of 0.01 and each of this value is compared with $\mathrm{i}_{\mathrm{L1ref}}$ and $\mathrm{i}_{\mathrm{L2ref}}$ during every sampling interval and the duty cycle which gives the least cost function value is selected. The working of the MPC controller is represented in below Figure 5.

4 Simulation Results

To validate the effectiveness of the proposed control strategy it is compared with a conventional PI-based control strategy. Firstly, a sudden change in load current is considered using a resistive load. Secondly, performance is evaluated with sudden change in source. Finally, reference change is given. Table 2 shows the simulation parameters and the simulation studies done on IBC with resistive load.

4.1 A Step-change in Load Demand

To analyse the performance of the proposed control strategy first step change in load demand is considered. Figure 6(a) shows the DC link voltage variation, Figure 6(b) shows output current response and Figure 6(c) shows inductor currents with conventional PI and proposed MPC control strategy. At 0.4 sec the load current is increased by decreasing the load resistance by 50% and at 0.8 sec the load current is decreased by increasing the load resistance by 50%. It is evident from Figure 6(a) that the proposed control strategy provides lesser overshoot, undershoot, and faster regulation with less settling time. At 0.4 sec and 0.8 sec, the DC link voltage settling time is 2.5 msec and 3 msec for proposed MPC and 30 msec and 14 msec for conventional PI controller respectively. At 0.4 sec and 0.8 sec, the peak overshoot is 0.85 V and 1.77 V for the proposed MPC. The peak overshoot for the conventional PI controller is 2.7 V and 4.4 V for the same.

Table 2 Simulation parameters

Symbol	Parameter	Value
V_{in}	Input voltage	20 V
L_1	Inductance	2 mH
L_2	Inductance	2 mH
R_L	Load resistance	1.9 Ω
V_o	Output voltage	6.5 V
C_0	DC Link capacitance	470 μF
T_h	Sampling period	0.1 ms
N	DC link voltgae horizon.	15
$\mathrm{k_p}, \mathrm{k_i}$	Inner current loop PI parameters	40,0.5
$\mathrm{k_p}, \mathrm{k_i}$	Inner current loop PI parameters	40,0.5
$\mathrm{k_{pv}}, \mathrm{k_{iv}}$	Outer voltage loop PI parameters	10,0.5
$\mathrm{f_s}$	Switching frequency	10 kHz

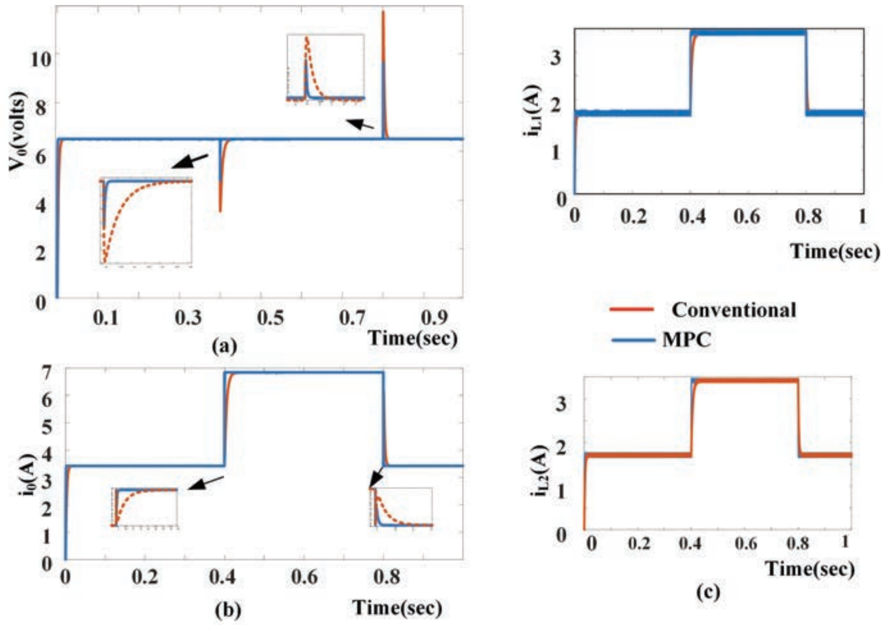

Figure 6 Simulation results for step change in load (a) DC link voltage (b) output current (c) inductor currents with conventional PI and proposed MPC method.

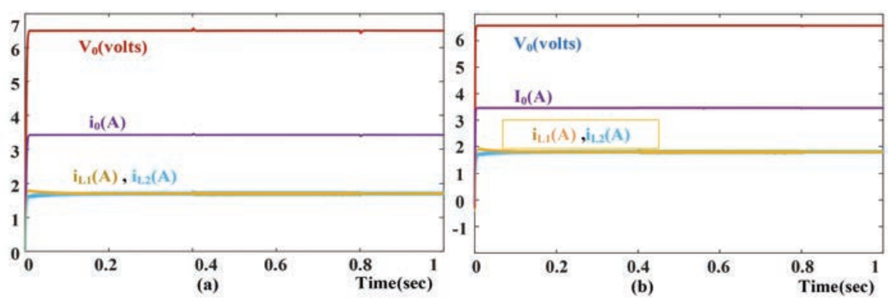

Figure 7 Simulation results for step change in source voltage (a) conventional PI control (b) proposed MPC control strategy.

4.2 Step Change in Source Voltage

Figure 7(a) and 7(b) illustrates step-change in source voltage with conventional PI control and proposed MPC strategy. At 0.4 sec, a step increase in the source is applied and at 0.8 sec, the step decrease in the source is applied. The DC bus voltage is settled at 6.5 V and corresponding output current is

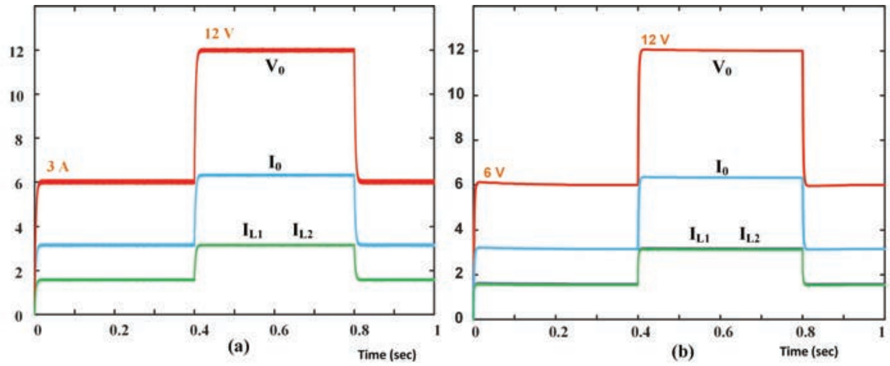

Figure 8 Simulation results for step change in reference voltage (a) conventional control (b) proposed MPC control strategy.

3.42 A and the inductor currents are 1.71 A. Due to the faster action of MPC, the DC bus voltage has lesser peak overshoot and faster settling time. Further, the load current is constant irrespective of the variation in source voltage and the inductors shared the current equally in all scenarios.

4.3 Step Change in Source Voltage

Figure 8(a) and 8(b) shows a step change in reference voltage with conventional PI control and proposed MPC respectively. At 0.4 sec, the reference voltage changes from 6 V to 12 V, and at 0.8 sec it is back to 6 V. The MPC tracks the change in reference voltage and regulates the DC bus voltage effectively. Due to the increase in load voltage, the load current increases from 3.15 A to 6.3 A and back to 3.15 A. Also, the inductors share the load current equally throughout the period. It is evident that the proposed MPC strategy shows faster tracking of reference voltage compared to the conventional PI control.

4.4 Comparison Between PI and MPC

The proposed MPC method is compared with a conventional PI-based IBC converter for further validation. Figure 6(a) shows the comparison between PI and MPC methods with load disturbance. As mentioned earlier, the MPC method shows faster DC bus voltage restoration and less peak overshoot. The settling time for PI is 15–30 msec and MPC is 2–3 msec. The summary is presented in bar diagram Figure 9.

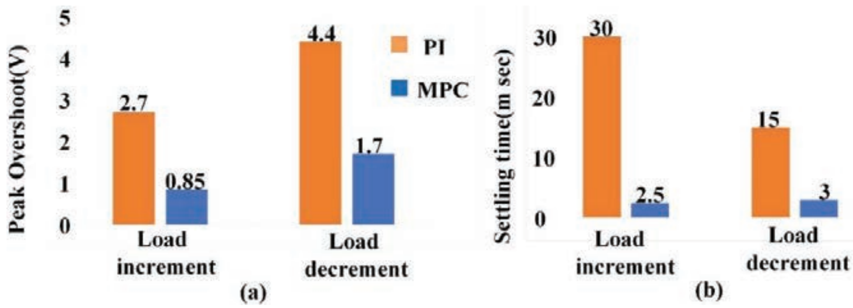

Figure 9 Comparison with PI and MPC during load increment and decrement (a) peak overshoot (b) settling time.

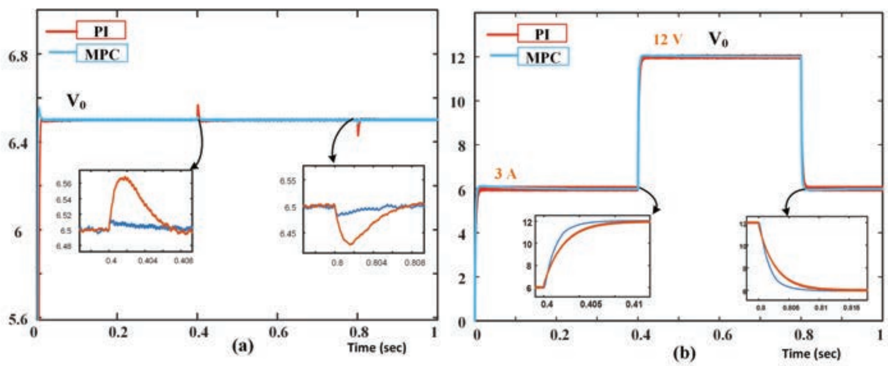

Figure 10 Comparison with PI and MPC during (a) source increment and decrement (b) reference change.

Further, the proposed method is compared with PI for source variation and reference variation as shown in Figure 10(a) and 10(b) respectively. For the PI method, the variation in load voltage is 70 mV for both increment and decrement. On the other hand, the variation for MPC based method for both scenarios is approximately 10 mV. The settling time for MPC is 2 msec and PI is 10 msec. A summary of source variations is represented in the bar diagram as shown in Figure 11. The reference is increased from 6 V to 12 V and brought back to 6 V after some time to verify the operation with the proposed controller. Compared to PI, the MPC tracks the reference quickly without any disturbance. The PI requires approximately 10–15 msec to reach the steady state and the proposed MPC method requires only 2–3 msec for reaching the final state during reference change. In short, the MPC-based method has faster settling and minimal peaks compared to the conventional PI-based method.

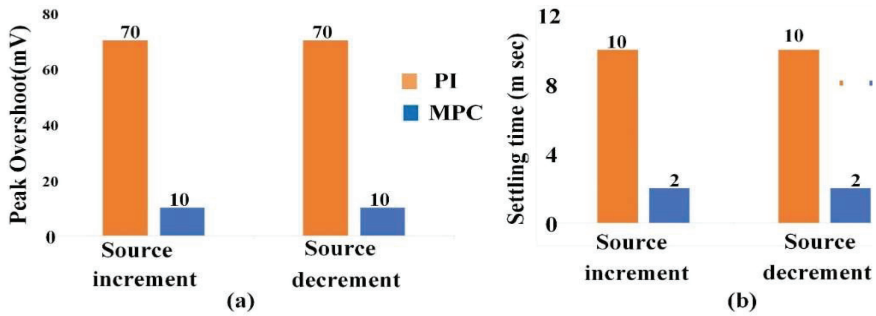

Figure 11 Comparison with PI and MPC during source increment and decrement (a) peak overshoot (b) settling time.

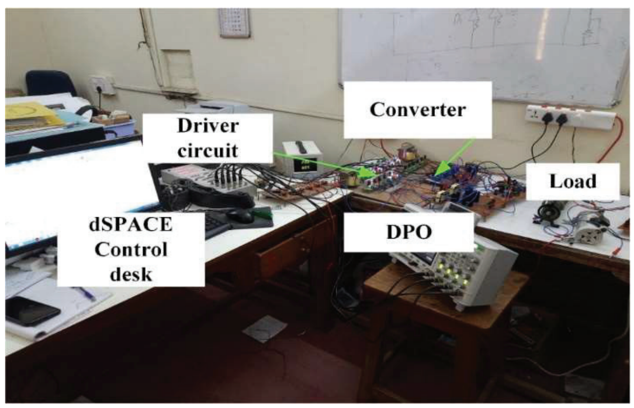

Figure 12 Prototype model of the proposed topology.

5 Experimental Results

To test the proposed control technique, a scaled-down experimental version is used, as shown in Figure 12. The controller is implemented with a dSPACE DS1104 and the IBC is realized with IRF540N MOSFETs. Table 3 shows the experimental parameters of system under consideration. The controller performance is evaluated using a step-change in load current, a step-change in source voltage, and a step-change in reference voltage. Finally, the experimental results of the proposed control are compared to those of the conventional control.

Primarily, the load variation is applied to verify the proposed controller. Figure 13(a) and 13(b) depicts step increase in load current and Figure 14(a) and 14(b) illustrate step decrease in load current with conventional PI and

Table 3 Experimental setup parameters

Symbol	Parameter	Value
V_{in}	Input voltage	20 V
V_o	Output voltage	6.5 V
L_1	Inductance	2 mH
L_2	Inductance	2 mH
R_L	Load resistance	16.5 Ω
C_0	DC Link capacitance	470 μF
T_h	Sampling period	0.1 ms
N	DC link voltage horizon	8
f_s	Switching frequency	10 khz

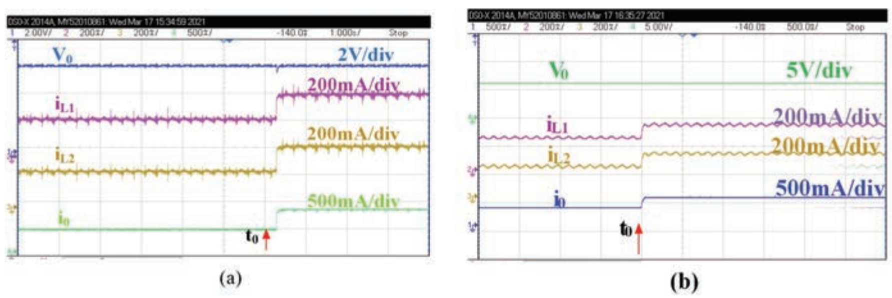

Figure 13 Experimental results for step increase in load current demand (a) conventional control (b) proposed MPC control strategy.

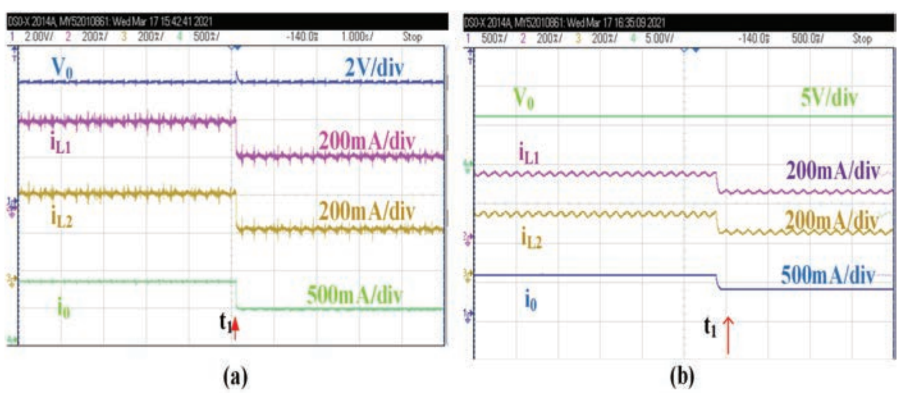

Figure 14 Experimental results for step decrease in load current demand (a) conventional control (b) proposed MPC control strategy.

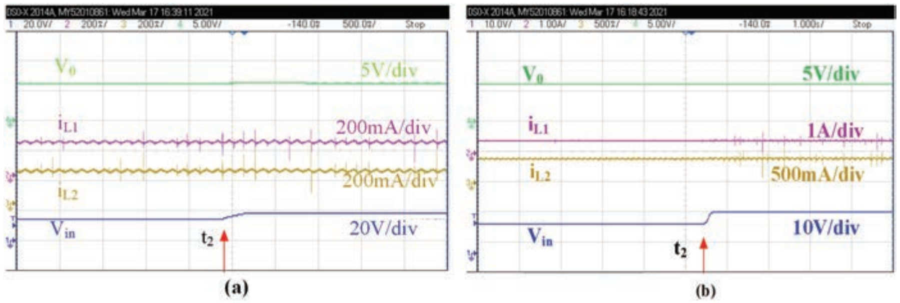

Figure 15 Experimental results for step increase in source voltage (a) conventional control (b) proposed MPC control strategy.

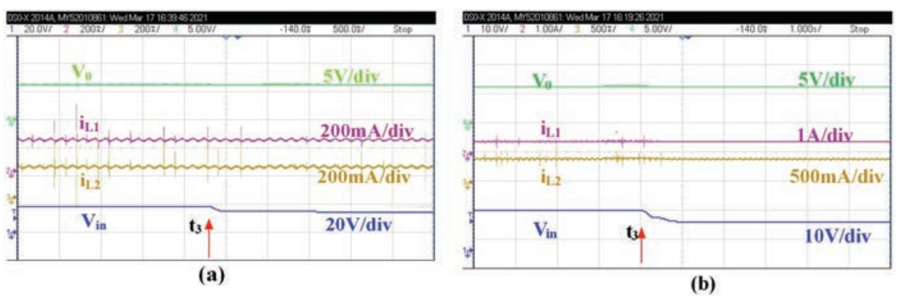

Figure 16 Experimental results for step decrease in source voltage (a) conventional control (b) proposed MPC control strategy.

proposed MPC respectively. At $t = t_0$ sec the load current is increased by decreasing the load resistance by 50% and at $t = t_1$ sec the load current is decreased by increasing the load resistance by 50%. The DC bus voltage is settled at 6.5 V and corresponding output current is 0.4 A and the inductor currents are 0.2 A. It is observed that there is an undershoot and overshoot in DC bus voltage with conventional PI and no significant voltage dip with proposed MPC. Also, it is relevant to note that the inductor currents have more ripples with PI controller and minimal ripple in the MPC method. The MPC method cancels out almost ripple currents in inductors.

Figure 15(a) and 15(b) illustrate step-change in source voltage with conventional PI and proposed MPC respectively. Figure 16(a) and 16(b) illustrates step decrease in source with conventional PI and proposed MPC. At the $t = t_2$ step increase in source, voltage is applied and at $t = t_3$ step decrease in source, voltage is applied. The DC bus voltage is settled at 6.5 V.

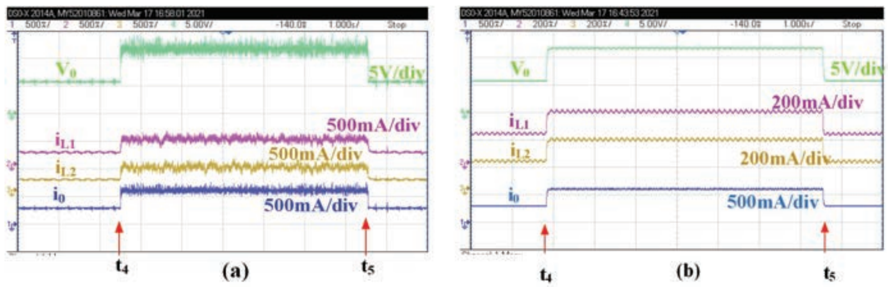

Figure 17 Experimental results for step change in reference voltage (a) conventional control (b) proposed MPC control strategy.

Further, the load current is constant irrespective of the variation in source voltage and the inductors shared the current equally in all scenarios.

In Figure 17(a) and 17(b) a step-change in reference is introduced. At $t = t_4$ reference voltage changes from 6 V to 12 V and $t = t_5$ is back to 6 V. The MPC tracks the change in reference voltage and regulates the DC bus voltage effectively. Due to the increase in load voltage, the load current increases from 0.36 A to 0.72 A and back to 0.36 A. Also, the inductors share the load current equally throughout the period. The PI-based IBC shows more DC bus voltage oscillations compared to MPC during reference change. The MPC can effectively handle the reference variation compared to PI. It is evident that the proposed MPC strategy shows faster tracking of reference voltage compared to the conventional PI control.

6 Conclusion

This paper compares a predictive control strategy for an interleaved buck converter to a conventional control strategy. Since the conventional control strategy employs a PI controller, the desired output cannot be achieved due to tuning issues and parameter dependence on the operating point. The key benefit of MPC is its flexibility, ease of execution, incorporation of constraints and nonlinearities. It predicts the system's future states using a discrete model and the system's current states. Three cases have been studied with resistive load. Firstly, sudden change in resistive load is used to achieve abrupt change in load current. Secondly, a sudden change in the source voltage is applied followed by a sudden change in reference voltage to see whether the proposed MPC controller tracks transitions faster than traditional PI controller. In each of these cases, relevant waveforms are presented along with simulation and experimental results and observed that the proposed control has improved dynamic and steady-state performance compared to the traditional one.

References

[1] Vijayalakshmi, S., E. Arthika, and G. Shanmuga Priya. "Modeling and simulation of interleaved Buck-boost converter with PID controller." 2015 IEEE 9th International Conference on Intelligent Systems and Control (ISCO). IEEE, 2015.

[2] Bhaskar, Mahajan Sagar, et al. "4Nx non-isolated and non-inverting hybrid interleaved multilevel boost converter based on VLSIm cell and cockcroft walton voltage multiplier for renewable energy applications." 2016 IEEE International Conference on Power Electronics, Drives and Energy Systems (PEDES). IEEE, 2016.

[3] Mao, Hong, et al. "Analysis of inductor current sharing in nonisolated and isolated multiphase dc–dc converters." IEEE Transactions on Industrial Electronics 54.6 (2007): 3379–3388.

[4] M. S. Bhaskar, D. J. Almakhles, S. Padmanaban, J. B. Holm-Nielsen, A. R. Kumar and S. O. Masebinu, "Triple-Mode Active-Passive Parallel Intermediate Links Converter With High Voltage Gain and Flexibility in Selection of Duty Cycles," in IEEE Access, vol. 8, pp. 134716–134727, 2020, doi: 10.1109/ACCESS.2020.3010594.

[5] Jain, Piyush Kumar, and Amit Kumar. "Interleaved DC to DC buck converter for low power application." 2015 International Conference on Energy, Power and Environment: Towards Sustainable Growth (ICEPE). IEEE, 2015.

[6] Miftakhutdinov, Rais. "Optimal design of interleaved synchronous buck converter at high slew-rate load current transients." 2001 IEEE 32nd Annual Power Electronics Specialists Conference (IEEE Cat. No. 01CH37230). Vol. 3. IEEE, 2001.

[7] Zhao, Zheng, et al. "Derivation, analysis, and implementation of a boost–buck converter-based high-efficiency PV inverter." IEEE Transactions on Power Electronics 27.3 (2011): 1304–1313.

[8] Hsieh, Yao-Ching, et al. "A Soft-Switching Interleaved Buck–Boost LED Driver With Coupled Inductor." IEEE Transactions on Power Electronics 37.1 (2021): 577–587.

[9] Shrud, Mohamed A., et al. “Modeling and simulation of automotive interleaved buck converter.” 2009 44th International Universities Power Engineering Conference (UPEC). IEEE, 2009.
[10] Yuan, Zhibao, and Haiping Xu. “Pulse power supply with faster response and low ripple current using inductive storage and interleaving technology.” CPSS Transactions on Power Electronics and Applications 5.1 (2020): 54–62.
[11] Wang, J. B., Chuang, S., “A study of the interleaved buck derived converters”, IEEE International Conference on Industrial Technology, ICIT 2006.
[12] Shrud, M. A., Kharaz, A., Ashur, A. S., Shater, M., Benyoussef, I. “A study of modeling and simulation for interleaved buck converter”, 1 Power Electronic & Drive Systems & Technologies Conference, PEDSTC 2010.
[13] Illic, M., Maksimovic, D. “Averaged switch modeling of the interleaved zero current transition buck converter”. IEEE Power Electronics Specialists Conference, PESC 2005.
[14] Neacsu, D. O., Bonnice W., Holmansky, E. “On the small-signal modeling of parallel/interleaved buck/boost converters”. IEEE International Symposium on Industrial Electronics, ISIE, 2010.
[15] Andressa C. Schittler, Douglas Pappis, Cassiano Rech, Alexandre Campos, Marco A. Dalla Costa, “Generalized State-space Model For The Interleaved Buck Converter” XI Brazilian Power Electronics Conference, 21 November 2011.
[16] Mohamed. A. Shrud, Ahmad Kharaz, Ahmed. S. Ashur, Mustafa Shater and Ismail Benyoussef, “A study of Modeling and Simulation for Interleaved Buck Converter” 2010 1st Power Electronic & Drive Systems & Technologies Conference (PEDSTC), 24 May 2010.
[17] S. Iturriaga-Medina, P.R. Martinez-Rodriguez, M. Juarez-Balderas, J.M. Sosa and C.A. Limones, “A buck converter controller design in an electronic drive for LED lighting applications” 2015 IEEE International Autumn Meeting on Power Electronic and Computing (ROPEC), 01 February 2016.
[18] Jorge Garcia, Antonio J. Calleja, Emilio López Corominas, David Gacio Vaquero, Lidia Campa, “Interleaved Buck Converter for Fast PWM Dimming of High-Brightness LEDs” IEEE Transactions on Power Electronics, vol. 26, no. 9, September 2011.
[19] Bęczkowski, Szymon, and Stig Munk-Nielsen. “Two phase interleaved buck converter for driving high power LEDs.” Proceedings of the 2011

14th European Conference on Power Electronics and Applications. IEEE, 2011.

[20] Prasanth, Sangani, et al. "Efficient Interleaved Buck Converter Driver for LED Applications." 2019 IEEE International Conference on Sustainable Energy Technologies and Systems (ICSETS). IEEE, 2019.

[21] Arunkumar, C. R., Udaya Bhasker Manthati, and Srinivas Punna. "Supercapacitor-based transient power supply for DC microgrid applications." Electrical Engineering (2021): 1–10.

[22] Punna, Srinivas, Udaya Bhasker Manthati, and Arunkumar Chirayarukil Raveendran. "Modeling, analysis, and design of novel control scheme for two input bidirectional DC-DC converter for HESS in DC microgrid applications." International Transactions on Electrical Energy Systems (2021): e12774.

[23] Arunkumar, C. R., Udaya Bhasker Manthati, and Punna Srinivas. "Accurate modelling and analysis of battery–supercapacitor hybrid energy storage system in DC microgrid systems." Energy Systems (2021): 1–19.

[24] Rodriguez, Jose, and Patricio Cortes. Predictive control of power converters and electrical drives. Vol. 40. John Wiley & Sons, 2012.

[25] Hredzak, Branislav, Vassilios G. Agelidis, and Minsoo Jang. "A model predictive control system for a hybrid battery-ultracapacitor power source." IEEE Transactions on Power Electronics 29.3 (2013): 1469–1479.

[26] Dehghanzadeh, Ahmad, et al. "Model predictive control design for DC-DC converters applied to a photovoltaic system." International Journal of Electrical Power & Energy Systems 103 (2018): 537–544.

[27] Mei, Yang, Xiaoqing Li, and Yuanyuan Qi. "A model predictive control method for three-level bi-directional DC-DC converter in renewable generation system." 2015 18th International Conference on Electrical Machines and Systems (ICEMS). IEEE, 2015.

[28] Quevedo, Daniel E., et al. "Model predictive control of an AFE rectifier with dynamic references." IEEE Transactions on Power Electronics 27.7 (2011): 3128–3136.

[29] Katnapally, Akhil, et al. "A predictive power management scheme for hybrid energy storage system in electric vehicle." International Journal of Circuit Theory and Applications (2021).

Biographies

Mahesh Babu Tirumalasetti received his B.Tech. degree in Electrical and Electronics Engineering from Gayatri Vidya Parishad College of Engineering(A), Visakhapatnam, India and Master's in Power Electronics and Drives from National Institute of Technology-Warangal, India in 2016 and 2021, respectively. His research interest are energy storage systems, power electronic converters, and model predictive control.

Udaya Bhsaker Manthati received B.Tech degree in electrical and electronics engineering and M.E. in Power Electronics & Drives in 2003 and 2006 and Ph.D. in electrical engineering in 2011. Since 2012, he has been working as Assistant professor in department of electrical engineering at National Institute of Technology-Warangal, India. In 2011, he worked as Assistant professor at Manipal University Jaipur-India. He was a research assistant at CITCEA-UPC, Spain during 2007–2011. His research interest include bi-directional DC-DC converters, power electronics application to micro grid and smart grid technologies, energy storage systems, digital control and synchrotrons power supplies. He is a recipient of SLL-UPC fellowship during 2007–2010.

Punna Srinivas received B.Tech degree in electrical and electronics engineering from JNTU, Hyderabad, India in 2006. The Masters (M.Tech) and Ph.D in Power Electronics and Drives from National Institute of Technology-Warangal, India in 2009 and 2021 respectively. Currently, he is working as Assistant Professor at BVRIT HYDERABAD College of Engineering for Women, Hyderabad, India. His research interests include design and modeling of DC-DC converters for Energy storage systems, DC microgrid integrated hybrid energy storage system for linear and non-linear control technique.

C. R. Arunkumar received B.Tech and M.Tech degree in Electrical and Electronics Engineering and Power Electronics and control from Mahatma Gandhi University Kottayam, Kerala in 2013 and 2016 respectively. He is presently working towards Doctoral Program from National Institute of Technology-Warangal, India. His research interests include DC microgrid, Hybrid Energy Storage systems and DC-DC converters.